

Design of a 2-DOF Low Power Microrobot

Sarah Bergbreiter

EECS245: Introduction to MEMS Design Final Project

12/18/2000

Abstract

A two degree-of-freedom microrobot is designed in the Berkeley 3-layer SOI/DRIE process. The microrobot uses electrostatic actuation to minimize power consumption. To create out-of-plane motion, which translates to lateral movement for the robot, a variation on a torsional resonator is used. For in-plane motion, the microrobot uses a simple electrostatic gap-closing actuator to pivot the microrobot leg around its axis. The resulting microrobot has legs that are $40\mu\text{m}$ high and can move at theoretical speeds of $2\text{mm}/\text{sec}$. The microrobot can also rotate at $1.5^\circ/\text{sec}$. Total power consumption given the 64 legs in a 1mm^2 piece of silicon is $1.46\mu\text{W}$.

Introduction

As technology enables products to become increasingly smaller, new methods of manufacturing and assembly must be considered. Systems built using microelectromechanical systems (MEMS) technology promise manipulation and assembly tools on the same scale as the parts they will be putting together. Microrobots made from MEMS components can potentially act as autonomous assembly stations for small-scale manufacture. Arrays of microrobots could even yield inexpensive, tiny transport mechanisms to precisely move parts under a microscope or in any other situation where ultra fine movement is needed.

Microrobots will naturally require some means of actuation in order to manipulate parts. However, unlike robots in the macro world, actuators are not available as off-the-shelf components. Previously designed microrobots and micromanipulators have made use of a wide variety of actuation schemes. Thermal actuators, which run high currents through silicon “legs” to bend them, are popular due to the large displacements and forces they achieve [1-3]. The first walking silicon microrobot used thermal actuation [2]. However, thermal actuators consume large amounts of power that would prohibit them from being used in an autonomous system. Electrostatic actuators, on the other hand, realize smaller forces and displacements but expend much less power [4-6].

This microrobot design focuses on providing a low power electrostatic solution, which will make autonomous microrobots feasible when used with current solar cell technology [7]. The design also adds a second degree-of-freedom, to make the microrobot more maneuverable, increasing the number of potential applications for the design.

Fabrication

Part of the attraction for building mechanical systems in silicon is that bulk fabrication methods have already been developed by the integrated circuit industry. By using established, standard processes to build MEMS technology, it is much simpler to build a library of parts. In addition, CAD tools can be developed to model these devices.

Keeping this fact in mind, the Berkeley 3-layer SOI/DRIE process was used to design this microrobot. Deep Reactive Ion Etching (DRIE) an SOI wafer can generate aspect ratios of 20:1. Using an SOI wafer with a top layer of $40\mu\text{m}$ SCS translates to structures $40\mu\text{m}$ in height and $2\mu\text{m}$ wide. The process uses two topside etches. The first etch defines a Low SCS layer where the height is determined by the timing of the etch. The second etch produces a High SCS layer where the height is determined by the total thickness of the SOI wafer’s top layer. A backside etch and subsequent release step allow structures to be released in the plane of the wafer.

Leg Design

The robot legs are based on a torsional actuation scheme to generate out-of-plane motion (Figure 1). Each leg consists of a narrow beam and paddle suspended by two orthogonal rods that act as the torsional springs. Each rod is $50\mu\text{m}$ long and the paddle is $80 \times 20 \mu\text{m}^2$. Each of these structures is defined by the Low SCS layer, which is usually $5\text{-}8\mu\text{m}$ in height. Etch holes are included in the paddle to assure its release from the oxide during the release etch. A High SCS $40\mu\text{m}$ “foot” lies on the opposite side of the springs and makes contact with the surface that the microrobot is on or the object being manipulated. Each leg is designed to occupy a total area of $100 \times 100 \mu\text{m}^2$.

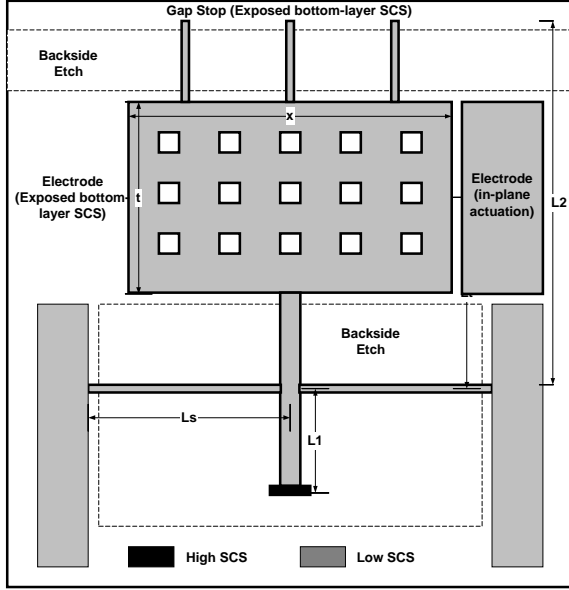


Figure 1. A top view of the 2-DOF leg. The electrode created by exposing the bottom layer of silicon is used for out-of-plane actuation, and the electrode to the right of the paddle is used for in-plane rotation.

In order to actuate the leg out of plane, a voltage is applied between the leg and an electrode beneath it. Exposing the bottom substrate of the SOI wafer creates an electrode that is electrically isolated from the top layer (Figure 2). The gap between the leg and electrode is defined by the thickness of the oxide in the SOI wafer and equals $2\mu\text{m}$. The voltage generates a downward electrostatic force, which deflects the paddle toward the electrode at an angle ϕ . This action also deflects the foot out-of-plane by the same angle. To prevent the actuator from pulling in, beams attached to the end of the actuator paddle act as a stop. By actuating the leg, the foot lifts the robot, which leads to movement when combined with the appropriate gait.

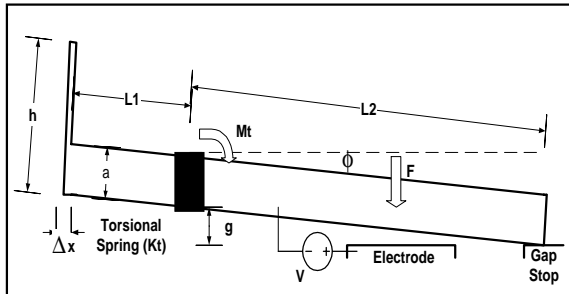


Figure 2. A voltage V is applied between the electrode and leg, which is supported by two torsional springs. The electrostatic force from the applied voltage causes the leg to move downward at angle ϕ .

In addition to the lateral movement initiated by the out of plane motion described, a second degree of

freedom is used to rotate the microrobot around its central axis. A separate and electrically isolated Low SCS actuator is placed on one side of the paddle. By applying a voltage between the side actuator and paddle, the paddle will pivot slightly around its intersection with the torsional springs. By combining the rotational in-plane movement with out-of-plane actuation, the robot can achieve rotational motion.

Out-of-Plane Actuation Analysis

Out-of-plane deflection for each leg is based on torsional actuation principles. The beams used to prevent the actuator from pulling in at high voltages provide a limit on the out-of-plane deflection angle that can be realized by the actuator, $\phi = \sin^{-1}(g/L_2)$. This maximum deflection angle in turn establishes the maximum lateral movement provided by the actuator, $\Delta x = h \cdot \sin \phi + L_1 (1 - \cos \phi)$. Assuming voltages that instantiate pull-in are applied, $\phi_{\text{max}} \approx 1.43^\circ$ and $\Delta x \approx 1\mu\text{m}$ for values $L_2 = 80\mu\text{m}$ and $g = 2\mu\text{m}$.

The effect of the torsional springs is examined to determine the minimum applied voltage required to achieve the desired angle for this design. The torque applied to the leg and the angle realized by this torque will be related by a torsional spring constant k_τ .

$$\tau = k_\tau \phi$$

From Beer and Johnston [8],

$$k_\tau = \frac{c_2 ab^3 G}{L}$$

L is given as the length of the torsional spring, a and b ($a > b$) define the cross section of the spring, and c_2 is a coefficient defined as a function of a/b found in [8]. G is the shear modulus of silicon, $G = E / 2(1+\nu)$. From [9], Young's Modulus for single crystal silicon, $E = 165\text{GPa}$ and Poisson's Ratio for single crystal silicon, $\nu = 0.22$, so the shear modulus $\approx 67.6\text{GPa}$. Using a conservative estimate for the thickness provided by the first etch, $a = 8\mu\text{m}$, $b = 2\mu\text{m}$, $L = 50\mu\text{m}$, and $c_2 = 0.281$, the torsional spring constant $k_\tau \approx 23.8 \text{ nN}\cdot\text{m}$.

When a voltage is applied to the electrode beneath the torsional actuator, it defines the torque about the torsional springs. Assuming the actuator is still parallel enough to use the parallel plate approximation for capacitance,

$$\tau = \int_A \frac{\epsilon_0 V^2}{2[g_0 - g(x)]^2} x dx$$

In this case, $g(x) = x \cdot \tan(\phi)$ and small angles allow a small angle approximation $\tan(\phi) = \phi$ to be used.

Equating the torque given by this expression with the restoring torque from the torsional spring, $k_\tau \phi$, the

resulting expression will lead to an appropriate voltage for the desired angle (Figure 3). Given the dimensions already discussed, a voltage of 50V should be sufficient to fully actuate each leg.

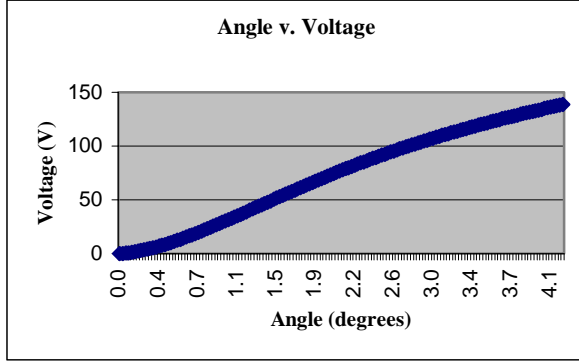


Figure 3. Applied voltage plotted against realized actuator angle.

In-Plane Actuation Analysis

The additional actuator added to deflect the leg around the torsional spring axis is modeled using the same gap closing actuator techniques applied in analyzing out-of-plane actuation. A more robust approach would take into account the transverse bending of the torsional beams in order for the foot to move appropriately on the opposite side, but this includes nonlinear effects that are not discussed in this paper. Instead, it is assumed that the beam and paddle act as any cantilever beam would,

$$\theta \approx \frac{1}{2EI} L^2 \left(\frac{1}{2} \epsilon_0 V^2 \frac{tx}{g^2} \right)$$

The beam is $8\mu\text{m} \times 4\mu\text{m}$ in cross section and will therefore have a relatively large spring constant $k_0 = 163 \text{ N/m}$. The forces required to rotate the beam by even a small angle will also be relatively large. Using the same 50V applied for out-of-plane actuation, $\theta \approx 0.0045^\circ$. It is currently assumed that the foot on the opposite side of the torsional springs will also deflect by this angle.

Power Analysis

The power requirement for each leg is an important factor in designing an autonomous microrobot. Because this is an electrostatic actuator, there is no current flow and power usage is minimal. Power is defined as

$$P = CV^2 f$$

The resonant frequency for a torsional actuator must consider the mass moment of inertia for the

actuator. By summing the individual mass moments for each component of the actuator, the mass moment of inertia for each leg is $I_m = 8.72e-20 \text{ kg}\cdot\text{m}^2$.

Resonant frequency for a torsional actuator is defined as

$$f_\tau = \frac{1}{2\pi} \sqrt{\frac{k_\tau}{I_m}}$$

Therefore, $f_\tau = 82\text{kHz}$ and the power consumption for out-of-plane actuation at approximately 1.25kHz in each leg is 22.13nW.

The resonant frequency for in-plane actuation is

$$f_\theta = \frac{1}{2\pi} \sqrt{\frac{k_\theta}{m}}$$

Given a mass of $3.5e-11 \text{ kg}$ for the beam and paddle, the resonant frequency, $f_0 = 343\text{kHz}$. By operating the in-plane actuator at only 333Hz, each leg consumes 0.59nW.

The 64 legs in this design will require $1.42\mu\text{W}$ of power for out-of-plane actuation using an $f_\tau = 1.25\text{kHz}$ and 37.8nW of power for in-plane actuation at $f_0 = 333\text{Hz}$. Therefore, the total power consumption in this microrobot design is $1.46\mu\text{W}$.

Robot Locomotion

Living organisms offer a large selection of locomotion methods for microrobots to choose from. Several insect-based designs have been proposed [4,5], and the ciliary motion of microorganisms has also been shown to work well [3]. Due to the leg design of this microrobot, a ciliary motion scheme is chosen as the best means for microrobot locomotion. The ciliary gait is described in Figure 4.

The speed that the microrobot can reach is easily found from multiplying the total movement that occurs during each full cycle by the frequency at which the leg is actuated, $v = f\Delta x$. As shown, each cycle provides a $2\Delta x$ lateral motion, and $\Delta x \approx 1\mu\text{m}$, giving a maximum speed of 2 mm/sec assuming an ideal contact model with the surface and a complete frequency of 1kHz (which translates to a frequency of 1.25kHz for each set of actuators).

Given two sets of independently driven out-of-plane leg actuators, A and B, where A can also be actuated in-plane, the following scheme should rotate the microrobot. Lift group B, rotate group A, lift group A, lower group B, rotate group A back to the original position, and lower group A. This scheme suggests a frequency for the in-plane actuators that is one third that of the out-of-plane actuators. Given a frequency of 333Hz for rotation, the microrobot will rotate $\approx 1.5^\circ$ each cycle.

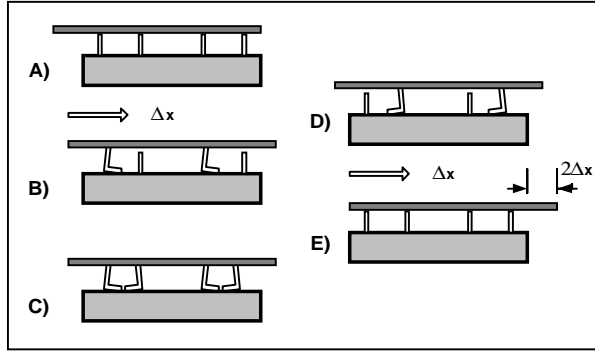


Figure 4. Placing the robot on its "back" demonstrates a total lateral movement of $2\Delta x$ achieved during each leg cycle. A) All of the robot legs are in the off state. B) The robot legs on the left side of each pair (Group A) are actuated, moving the object to the right Δx . C) The robot legs on the right side of each pair (Group B) are also actuated and come into contact with the object. D) Group A is turned off, and the object is held in place by the remaining actuated legs. E) Group B is turned off, moving the object to the left Δx .

In order for locomotion to be useful, the microrobot must be able to support at least its own weight. It was previously found that the torque provided by each out-of-plane actuator is approximately $594\mu\text{N}\cdot\mu\text{m}$. This translates into a force from each $40\mu\text{m}$ high foot of $29.7\mu\text{N}$. A microrobot with 64 legs in an area of 2.25mm^2 will support a force per unit area of $845\mu\text{N}/\text{mm}^2$. The weight of robot itself is $6.8\mu\text{N}/\text{mm}^2$ under the force of gravity, so these actuators provide more than enough force for the robot to support itself.

Conclusions

This paper presents a low power realistic alternative for microrobots. By using electrostatic actuation instead of the thermal actuators used in previous microrobots, power consumption is on the microwatt scale for a 2.25mm^2 design. Thermally actuated microrobot/microconveyer systems usually require power in the tens to hundreds of milliwatt range [1].

Experimentation and testing of the design and principles discussed still needs to be done. For example, it will be necessary to test the frictional and adhesive effects that are present at the contact point between the microrobot foot and surface. It is unlikely that the theoretical results for speed presented here will be practical in a real environment. A better model for in-plane actuation can be developed to take into account the nonlinear effects from the torsional springs. Test structures have been included in the current design layout to further investigate this question. The design parameters can

also be optimized to provide the most force output and speed in a given area of silicon.

It would also be interesting to integrate the solar cells developed in a complimentary SOI process with this design to create a completely autonomous microrobot. Experimenting with various designs given these criteria could lead to a simple, low power, autonomous microrobot.

References

- [1] P. E. Kladitis, V. M. Bright, Prototype microrobots for micro-positioning and micro-unmanned vehicles, Sensors and Actuators A: Physical 80 (2000) pp 132-137.
- [2] T. Ebefors, J. U. Mattsson, E. Kälvesten, G. Stemme, A walking silicon micro-robot, Transducers '99, Sendai, Japan (June 7-10 1999) pp 1202-1205.
- [3] J. W. Suh, R. B. Darling, K.-F. Böhringer, B. R. Donald, H. Baltes, G. T. A. Kovacs, CMOS integrated Ciliary actuator array as a general-purpose micromanipulation tool for small objects, Journal of Microelectromechanical Systems, 8 (4) December 1999 pp 483-496
- [4] K. Suzuki, I. Shimoyama, H. Miura, Insect-model based microrobot with elastic hinges, IEEE/ASME Journal of Microelectromechanical Systems 3 (1) 1994 pp 4-9.
- [5] R. Yeh, K. S. J. Pister, Design of low-power silicon microrobots, Proc. International Conference on Robotics and Automation, Workshop on Mobile Micro-Robots, April 2000, pp 21-28.
- [6] K.-F. Böhringer, B. R. Donald, R. Mihailovich, N. C. MacDonald, A theory of manipulation and control for microfabricated actuator arrays, Proceedings of the IEEE Workshop on Micro Electro Mechanical Systems (MEMS), January 1994, pp 102-107.
- [7] C. Bellew, Solar Cells +, <http://mems.me.berkeley.edu/~cbellew/overview.html>
- [8] F. P. Beer, E. R. Johnston, Jr. Mechanics of Materials, Second Edition, 1992.
- [9] MEMS Material database: <http://mems.isi.edu/mems/materials/index.html>